OXFORD UNIVERSITY PRESS | Tree Physiology

Radial growth phenology exposes diffuse-porous species to lower water availability than ring-porous and coniferous trees

Journal:	*Tree Physiology*
Manuscript ID	Draft
Manuscript Type:	Research Paper
Date Submitted by the Author:	n/a
Complete List of Authors:	D'Orangeville, Loïc; University of New Brunswick Fredericton, Faculty of Forestry and Environmental Management Itter, Malcolm Kneeshaw, D.; UQAM, Munger, William; Harvard University Richardson, Andrew; Northern Arizona University, Center for Ecosystem Science and Society and School of Informatics, Computing and Cyber Systems Dyer, James Orwig, David; Harvard Experimental Forest Pan, Yude; United States Department of Agriculture Forest Service Northern Research Station Pederson, Neil; Harvard Forest, Harvard Forest
Keywords:	growth rate, leaf phenology, radial growth, ring-porous, seasonality, Bud Break

Radial growth phenology exposes diffuse-porous species to lower water availability than ring-porous and coniferous trees

Loïc D'Orangeville[1,2], Malcolm Itter[3,4], Dan Kneeshaw[5], J. William Munger[6], Andrew D. Richardson[7,8], James M. Dyer[9], David A. Orwig[1], Yude Pan[10], Neil Pederson[1]

[1]Harvard Forest, Harvard University, Petersham, MA, 10366, USA.

[2]Faculty of Forestry and Environmental Management, University of New Brunswick, Fredericton, NB, E3B 5A3, Canada.

[3]Research Center for Ecological Change, University of Helsinki, Finland.

[4]Department of Environmental Conservation, University of Massachusetts Amherst, Amherst MA 01003, USA.

[5]Center for Forest Research, Université du Québec à Montréal, Montréal, QC, H3C 3P8, Canada.

[6]School of Engineering and Applied Sciences and Department of Earth and Planetary Sciences, Harvard University, Cambridge, MA 02138, USA.

[7]School of Informatics, Computing, and Cyber Systems, Northern Arizona University, Flagstaff, AZ 86011, USA.

[8]Center for Ecosystem Science and Society, Northern Arizona University, Flagstaff, AZ 86011, USA.

[9]Department of Geography, Ohio University, Athens, OH 45701, USA.

[10]U.S. Department of Agriculture Forest Service, Newtown Square, PA 19073, USA.

Corresponding author: Loïc D'Orangeville. Email: loic.dorangeville@unb.ca; telephone: 001-506-458-7232.

Keywords: radial growth; wood porosity; dendrometer band; temperate forest; water deficit; diffuse-porous; ring-porous.

Abstract

Climate models project warmer summer temperatures will increase the frequency and heat severity of droughts in temperate forests of Eastern North America. Hotter droughts are increasingly documented to affect tree growth and forest dynamics, with critical impacts on tree mortality, carbon sequestration, and timber provision. The growing acknowledgement of the dominant role of drought timing on tree vulnerability to water deficit raises the issue of our limited understanding of radial growth phenology for most temperate tree species.

Here, we use well-replicated dendrometer band data sampled frequently during the growing season to assess the growth phenology of 610 trees from 15 temperate species over six years. Patterns of radial growth follow a typical logistic shape, with growth rates reaching a maximum in June, and then decreasing until process termination. On average, we find that diffuse-porous species take 16-18 days less than other wood-structure types to put on 50% of their annual increment. However, their peak growth rate occurs almost a full month later than ring-porous and conifer species (ca. 24±4 days; mean±95% credible interval). Unlike other species, stem growth phenology of diffuse-porous species in our dataset is highly correlated with their spring foliar phenology.

When we match each species' period of rapid growth with water availability during the six-year study period, we find that delayed stem phenology in diffuse-porous species exposes them to higher water deficit of 88±19mm (mean±SE) than ring-porous and coniferous species (15±35 mm and 30±30 mm, respectively). Considering the high climatic sensitivity of wood formation observed here, our findings highlight our poor ecological understanding of wood growth phenology drivers. The later window of growth in diffuse-porous species coinciding with

peak evapotranspiration and lower water availability could reveal to be a potential mechanism behind recent reports of higher drought sensitivity in diffuse-porous species.

Introduction

Global change represents a growing threat for many dominant processes that drive the dynamics of forests (Bonan, 2008). Among these processes, wood growth controls ecosystem carbon (C) sinks (Pan *et al.*, 2011), timber production, and is closely related to other demographic processes like mortality and fecundity (Wyckoff & Clark, 2000, 2002; Berdanier & Clark, 2016; Buechling *et al.*, 2017; Cailleret *et al.*, 2017). A growing number of studies document climate change impacts on tree growth related, in particular, to increased water deficits under global warming (Dai, 2013; Cook *et al.*, 2015). Negative impacts of water deficit on tree growth and health has been shown to vary according to a wide array of stand-level conditions including soil characteristics (Buckland *et al.*, 1997; West *et al.*, 2012; Phillips *et al.*, 2016), stand diversity (Grossiord, 2018), local precipitation and evaporative demand (Williams *et al.*, 2013; McDowell & Allen, 2015; D'Orangeville *et al.*, 2018), and competition for resources (Martin-Benito *et al.*, 2011; D'Amato *et al.*, 2013; Gleason *et al.*, 2017; Bottero *et al.*, 2017). In addition, many tree-level traits also affect individual vulnerability under altering environmental conditions such as carbon allocation strategies (Trugman *et al.*, 2018), previous disturbance history (Itter *et al.*, 2019), rooting depth (Padilla & Pugnaire, 2007; Phillips *et al.*, 2016), water-use efficiency (Peters *et al.*, 2018), or wood structure (Elliott *et al.*, 2015; Kannenberg *et al.*, 2019). Multiple studies also suggest that larger trees may be more vulnerable to drought with serious implications for carbon sequestration (Bennett *et al.*, 2015). Despite this ever-growing understanding, the vulnerability of forests to hotter droughts remains uncertain and may be greatly underestimated (Allen *et al.*, 2015).

The timing of drought may strongly influence on the drought vulnerability of trees, due to the highly seasonal nature of cambial activity (i.e. wood cell division and enlargement) and its acute sensitivity to water availability (Gruber *et al.*, 2010; Foster *et al.*, 2014; Lempereur *et al.*, 2015). Recent observations at the global scale (Huang *et al.*, 2018) as well as in dry Mediterranean forest systems (Forner *et al.*, 2018) support these general concepts. In temperate forests of Eastern North America, drought impacts on current-year radial growth were reported to reach their peak in June (D'Orangeville *et al.*, 2018; Kannenberg *et al.*, 2019), coinciding with the period of maximal cambial activity (Rossi *et al.*, 2006b; Deslauriers *et al.*, 2007; D'Orangeville *et al.*, 2018). This relatively short seasonal window for cambial cell differentiation is mainly driven by climate (Rossi *et al.*, 2008b), but may also be modified by water deficit (Gruber *et al.*, 2010; D'Orangeville *et al.*, 2013a). Tree size and canopy position have also been reported to affect radial growth phenology. In timberline conifer stands, older and larger trees display a shorter growing period (Rossi *et al.*, 2008a) while in temperate stands, overstory fir trees start their growth earlier and end it later than understory trees (Rathgeber *et al.*, 2011). Species differences in wood structure also have a large influence on the phenology of radial growth. Earlier cambial reactivation and wood cell lignification in ring-porous species relative to diffuse-porous species was first reported in a temperate forest in England (Priestley & Scott, 1936). This pattern has since been documented in other temperate forests of Europe (Barbaroux & Bréda, 2002) and Asia (Takahashi *et al.*, 2013), and in the Acadian forest of North America (Lavigne *et al.*, 2004). Earlier growth in ring-porous species is likely due to the winter embolism of their large xylem vessels requiring restoration of the water transport pathway before leaves can unfold and begin transpiring (Zimmermann & Brown, 1971; Sperry *et al.*, 1994). Differences in phenology may explain why the radial growth of ring-porous *Quercus robur* and *Q. rubra* in Belgium is more sensitive to spring droughts while the diffuse-porous species *Fagus sylvatica* reacts more strongly to summer drought (Vanhellemont *et al.*, 2019). Accounting for the seasonal window of climate sensitivity in secondary growth, which appears distinct from that of leaf phenology (Seftigen *et al.*, 2018), may significantly improve our ability to predict future changes in forest productivity. However, our comprehension of radial growth phenology is limited for most temperate species, and nearly all eastern North American species (Delpierre *et al.*, 2016).

Contrary to stem growth phenology, leaf phenology is more easily measured using non-intrusive techniques like cameras (Richardson, 2019) or repeated seasonal observations (Denny *et al.*, 2014). Monitoring radial growth phenology requires more time-consuming approaches. Cellular monitoring uses frequent collection of wood samples and extensive laboratory processing, leading to low sample replication. To date, intensive cambial phenology investigations have been mainly applied to coniferous species from boreal and alpine ecosystems (Rossi *et al.*, 2006a; Deslauriers *et al.*, 2008; D'Orangeville *et al.*, 2013b). Dendrometer bands, permanently attached to trees, offer a low-cost method to monitor stem radial growth over a large number of trees. While mostly used to study annual growth, they have been shown to provide valuable estimates of intraseasonal growth dynamics and phenology (Deslauriers *et al.*, 2007) using reproducible methods that can be reproduced across trees, species, and sites (McMahon & Parker, 2015). Here, we utilized a dendrometer band network comprising 610 trees in a secondary-growth, temperate mesic forest to provide a first comparison of radial growth phenology between 15 different tree species in the northeastern US. Our objectives were 1) to identify the main drivers of seasonal radial growth phenology in diffuse-porous, ring-porous and non-porous tree species spanning a wide array of sizes and levels of vigor and 2) to relate stem phenology to leaf phenology and seasonal climate, specifically seasonal variations in water deficit.

Materials and Methods

Site Location

This study uses a six-year data collection (1998-2003) from within the footprint of the Environmental Measurement Site (EMS) eddy-covariance flux tower at the Harvard Forest in central Massachusetts, USA (42°30′ N, 72°10′ W). The Harvard Forest is a mixed deciduous broadleaf-dominated forest located in the temperate mesic region of Eastern North America with stony to sandy loam soils derived from glacial till. Forests are dominated by northern red oak (*Quercus rubra* L.) and red maple (*Acer rubrum* L.), with a smaller representation of American beech (*Fagus grandifolia* Ehrh.), eastern hemlock (*Tsuga canadensis* L. Carrière), eastern white pine (*Pinus strobus* L.), and yellow birch (*Betula alleghaniensis* Britton). Climate in the study area is temperate continental, with warm summers (19°C in July) and cold winters (on average -12°C in January). Mean annual precipitation is 1120 mm, a total that is rather evenly distributed over the year. On-site weather records indicate that the study period included the driest summer (1999) over a 26-year period (1991-2017), with monthly precipitations of 52 mm relative to a monthly average of 111 mm from June to August. The last two decades, however, represent a regional wet period with increased frequency of rainfall events during the summer (Bishop & Pederson, 2015).

Forty circular, 10-m radius biometric plots were randomly placed during the summer of 1994 within 100-m increments along eight 500-m transects that extended from the EMS eddy-flux tower (Fig. 1). All live trees of diameter at breast height (DBH) greater than or equal to 10 cm were tagged and their DBH measured. Six plots that became flooded by a beaver pond or were affected by selective harvest operation in 2001 have been excluded from analysis. In 1998, the tagged trees were resampled and manual dendrometer bands were installed (Barford *et al.*, 2001). From 1998 to 2003, gap increments in dendrometer bands were recorded approximately every 1-2 weeks during the growing season using digital calipers (resolution ~0.01 mm). During this period, 881 trees were monitored across 34 plots, including three ring-porous species (white ash, *Fraxinus americana* L.; northern red oak; black oak, *Quercus velutina* Lam.), four conifers (white spruce, *Picea glauca* (Moench) Voss.; red pine, *Pinus resinosa* Aiton; eastern white pine; eastern hemlock), and eight diffuse-porous species (striped maple, *Acer pennsylvanicum* L.; red maple; yellow birch; black birch, *Betula lenta* L.; white birch, *Betula papyrifera* Marshall.; grey birch, *Betula populifolia* Marshall.; American beech; black cherry, *Prunus serotina* Ehrh). All species but striped maple were found in multiple plots, with red maple, northern red oak and eastern hemlock being the most common species (36%, 21% and 13% of sampled trees, respectively).

Modelled growth phenology

Dendrometer measurements were converted to an arc to account for the circular nature of the dendrometer band, using measured tree DBH, then translated into diameter values. After removal of tree-years with less than 10 measurements during the growing season, 52,512 diameter measurements were used for modelling, corresponding to 3,286 tree-years spread over 698 trees (on average five year of data per tree). A five-parameter logistic model was fitted using an existing function for the R statistical computing environment on each set of intra-annual growth values (McMahon & Parker, 2015):

$$dbh_{doy} = \frac{K - L}{1 + {}^{1}/_{\theta} * \exp\left(-r(doy - doy_{ip})/\theta\right)^{\theta}}$$

Where dbh_{doy} is the measured DBH, r represents the maximum growth rate, L and K are initial and end-of-year DBH, doy_{ip} is the day of year (doy) when maximum growth rate occurs, and θ is a tuning parameter adjusting the approach to the upper asymptote. Given the fitted function provides accurate characterization of growth, but less accurate starting and ending diameter sizes, a likelihood ratio test was used to further constrain the estimation of these values following (McMahon & Parker, 2015). Following a preliminary analysis that indicated growth rates peaked in June (see Results), we noted that the lower early-season sampling effort – compared to the frequency of sampling later in the season – impeded the model capacity to accurately estimate the initial diameter value. To avoid this potential bias as well as the confounding effect of stem rehydration in the spring (Kozlowski & Winget, 1964; Deslauriers *et al.*, 2007), the upper asymptote from the prior-year model was used as the starting diameter of a tree. We therefore excluded from our analysis each tree's first-year intra-annual model (743 out of 3,286 tree-years, i.e. 23% of all tree-years).

Negative or null growth was detected in 9% of the annual observations. They were disproportionately associated with red maple trees (55% of observations), while no other species comprised more than 8% of such observations. Observations of trees with no growth were excluded from the analysis. Another 11% of the annual growth models displayed poor fits with abnormal model parameters (e.g. winter growth peak, staircase growth increments) and were excluded. The large majority of these poor fits were represented by small, suppressed trees with low growth rates potentially confounded with stem swelling and shrinking or measurement uncertainty. Indeed, 82% of these trees displayed lower-than-average vigor, and 67% displayed lower-than-average aboveground biomass. The final dataset used in the analysis contains up to five years of growth for 610 trees from 15 species distributed across 34 plots, for a total of 1,992 models (Table 1). The most abundant species were red maple, northern red oak, and Eastern hemlock. On average, each tree was represented with four years of growth.

Growth models fitted using frequently collected dendrometer data provide accurate predictions of the main period of stem radial growth due to both high sampling frequency and high growth rates (Deslauriers *et al.*, 2007). The use of dendrometers to determine the onset and cessation of secondary growth is much less accurate, because of the low growth rates and potentially confounding effects of stem swelling and shrinking (Tardif *et al.*, 2001; Deslauriers *et al.*, 2003). We, therefore, limited our analysis to the seasonal window of rapid growth. Three phenological indices were derived from individual growth models: W25, W50 and W75, which correspond to the day of year when 25, 50 and 75% of cumulative annual stem radial growth is reached, respectively (Fig. 2).

Bud break phenology

During the same sampling years (1998-2003), bud and leaf characteristics were documented at 3-7 day intervals from April to June on one to five permanently tagged understory and overstory individuals outside of the study plots but within a 1.5-km radius (Richardson & O'Keefe, 2009). The monitored species comprised all species with manual dendrobands except red pine and white spruce. We interpolated the timing of bud break and leaf development for each tree and each year. Bud break was defined as the occurrence of 50% of the buds on an individual having recognizable emergent leaves, while leaf development was defined as the occurrence of at least 75% of the leaves on an individual having reached 75% of their final (mature) size. This point was used rather than "fully developed" because the leaves are functional but still developing rapidly during this period, which permits better estimation of a date between observations.

Tree characteristics

Cambial growth rates and tree size can impact the beginning, duration and end of stem growth (Rathgeber *et al.*, 2011). We used the logistic growth model to interpolate the dendrometer data over time, and generate fine temporal resolution estimates of tree DBH. We converted these estimates to aboveground biomass estimates using species-specific allometric equations (Smith & Brand, 1983; Jenkins *et al.*, 2004). Tree vigor was calculated as the ratio of modelled annual biomass increment over tree biomass at the start of the growing season.

Climate

Daily temperature and precipitation were measured at the Harvard Forest weather station. Radiation prior to 2002 did not include global horizontal irradiance (GHI), required by our model to predict potential evapotranspiration (PET), a measure of moisture demand. Half-hourly radiation date was therefore extracted for the study site (4-km resolution) from the National Solar Radiation Data Base (Physical Solar Model 2(Sengupta *et al.*, 2018). The Turc algorithm was used to compute daily PET based on temperature and radiation data (Dyer, 2009). A Climate Moisture Index (CMI) was then calculated by subtracting PET from daily precipitation.

Analysis

A multivariate mixed model was used to estimate the effects of wood structure, tree size and vigor on the phenological indices W25, W50 and W75. The inclusion of size and vigor in the model allowed us to control for potential biases induced by the larger average size of ring-porous trees compared to non-porous and diffuse-porous species (Table 1). Specifically, the joint phenological response defined as $\boldsymbol{y}_{it} = (W25_{it}, W50_{it}, W75_{it})'$ where i and t index the individual tree and year of the observation respectively ($i = 1,2,\ldots,n; t = 1,2,\ldots,T$), was modeled using a multivariate normal likelihood. Note that each $\boldsymbol{y}_{it}$ corresponds to vector of length three, the total number of phenological indices. The effects of species, year, and sample plot were controlled for by including each variable as an additive random effect to the mean response. Specifically for each observation,

$$\boldsymbol{y}_{it} = \mathbf{B}\mathbf{x}_{it} + \mathbf{u}_{i(s)}^{(\text{species})} + \mathbf{u}_{t}^{(\text{year})} + \mathbf{u}_{i(l)}^{(\text{plot})} + \boldsymbol{\epsilon}_{it},$$

where $\mathbf{B}\mathbf{x}_{it}$ defines the fixed effects in the model ($\mathbf{x}_{it}$ includes observations of wood structure, tree size, and tree vigor, while $\mathbf{B}$ includes three sets of regression coefficients for each covariate—one for each phenological index), the $\mathbf{u}$ terms define species, year, and plot random effects (note, $s(i)$ and $l(i)$ indicate the species and plot corresponding to the ith tree), and $\boldsymbol{\epsilon}_{it}$ is the residual error, $\boldsymbol{\epsilon}_{it} \sim Normal(\mathbf{0}, \Sigma)$, where Σ is a 3-dimensional covariance matrix.

Model parameters were estimated as part of a broader Bayesian hierarchical framework (Gelman *et al.*, 2013). Additional information on the prior distributions and Bayesian inferential approach including the MCMC sampler is provided in the Supplementary Information Note S1.

Results

Stem growth phenology

Averaged across trees and years, model-derived stem growth rates peaked on June 19, with interannual variability ranging between June 10 (in year 2001) and June 25 (in year 2003; 95% credible interval, $CI_{95\%}$: 0.001 to 0.06 mm·day^{-1}; Fig. 3). However, we observed large variations in the phenology of growth among trees based on their wood structure, with conifers (i.e., non-porous species) and ring-porous oaks having consistently earlier windows of peak stem growth than diffuse-porous black cherry, American beech, birches, and maples (Fig. 3).

Bud break in diffuse-porous species precedes the modelled 25% stem growth threshold by an average of 36±6 days. In contrast, bud break in ring-porous species is simultaneous with their 25% stem growth threshold (within 3±7days), while conifer leaf phenology lags behind it by 26±7 days on average (Fig. 3).

Controlling for size and vigor differences across trees as well as random plot, year, and species effects, our multivariate model confirms the observed striking difference in growth phenology with wood structure: on average, diffuse-porous trees completed 25% of their annual stem growth later than coniferous and ring-porous trees by 29 days ($CI_{95\%}$:14-43) and 35 days ($CI_{95\%}$: 20-51), respectively (Fig. 4). These differences diminish over the growing season due to higher growth rates in diffuse-porous trees: they completed 75% of their stem growth later only 12 days ($CI_{95\%}$:0-27) and 17 days later ($CI_{95\%}$: 3-33) than coniferous and ring-porous species, respectively. Such pattern results in diffuse-porous species having higher growth rates during the period of 25 to 75% of annual growth and a shorter duration in peak stem growth period versus coniferous and ring-porous species, lasting only 38 days ($CI_{95\%}$:25-52) in diffuse-porous species, compared to 54 days ($CI_{95\%}$:39-69) and 56 days ($CI_{95\%}$:39-72) in coniferous and ring-porous species, respectively (Fig. 4).

Compared with wood structure, our multivariate model indicates relatively smaller effects of biomass and vigor on the seasonality of stem growth (Fig. 5). The peak stem growing period of larger and more vigorous trees tends to extend later in the season, but only by a few days. Controlling for all other variables including wood structure, largest trees completed 25, 50 and 75% of their annual stem growth on an average of 9, 6, and 5 days later than the smallest trees, respectively (Fig. 5). Similarly, the most vigorous trees completed 25, 50 and 75% of their annual stem growth only 14, 10 and 7 days later than the slowest-growing trees, respectively.

Linking stem growth with leaf phenology

The five diffuse-porous species used in this analysis display large, positive correlations between leaf and stem growth phenology across years (Fig. 6). The largest correlations are observed between bud break and the point when 25% of annual stem growth is completed (W25). These relations are equally strong within and across diffuse-porous species. Intra-species Pearson correlations range between 0.64 (white birch) and 0.95 (black birch), while correlation across all diffuse-porous trees reaches 0.81. The correlations between bud break and stem growth tend to diminish over the season in diffuse-porous trees, with correlations of 0.69 for W50 and 0.39 for W75. High correlations are also observed between leaf development (i.e. when at least 75% of the leaves on an individual have reached 75% of their final size) and stem growth in diffuse-porous trees, although the largest correlations are observed for W50 ($r=0.83$) and W75 ($r=0.81$) rather than W25 ($r=0.69$; Fig. 6). In contrast to diffuse-porous species, we observe a weaker relationship between leaf and stem phenology in ring-porous trees. Despite a relatively simultaneous bud break with W25, overall correlations for ring-porous species range between 0.30 and 0.52. The limited leaf phenology data did not allow for a robust assessment of this relationship for coniferous species, although there does not appear to be any visible synchrony (Fig. 6).

Stem growth phenology and seasonal water balance

Striking differences in moisture stress were observed during peak growth according to wood structure. Diffuse-porous trees were subject to a higher water deficit during their period of peak stem growth compared to ring-porous and coniferous trees (29±17 mm vs 0±19 mm and 5±18 mm, respectively; values are mean±SE). In addition, diffuse-porous trees were the only group of species with negative CMI during all five years of study (Fig. 7). This trend for reduced moisture availability in diffuse-porous species is likely related to their later seasonal window of peak stem growth, occurring concurrently with seasonal peaks in evapotranspiration (Fig. 7). For context, these relations occurred during substantially high interannual variation in moisture, documented here with the CMI (see Methods). The annual sum of weekly negative CMI, calculated here as the cumulative annual water deficit, ranged between 232 mm (year 2003) and 409 mm (year 1999; Fig. 7).

Discussion

Differences in cambial phenology on stand-scale processes like seasonal carbon sequestration and drought vulnerability remain poorly studied despite their important repercussions. Here, we found a significant later window of peak growth in diffuse-porous species versus ring-porous and non-porous species. Maples, birches, and other diffuse-porous species complete 25% of their stem growth ca. one month later than other species, but the delay in cambial growth is partially compensated by higher growth rates, so that diffuse-porous species complete 75% of their stem growth only two weeks later than other species.

The later window of peak growth in diffuse-porous species derives from physiological differences in reactivation in the region of the cambium. In diffuse-porous trees, the first vessels are formed when leaves are developing or mature, while the first vessels of ring-porous species are formed several weeks before bud break (Larson, 1962, 1994; Suzuki *et al.*, 1996; Barbaroux & Bréda, 2002; Zweifel *et al.*, 2006; Sass-Klaassen *et al.*, 2011; Takahashi *et al.*, 2013). The mechanisms driving these difference have been studied for a long time (Wareing, 1951), but are still debated (Frankenstein *et al.*, 2005). Auxin (indole-3-acetic acid) is an important promoter of cambium reactivation and has long been thought to originate from developing leaves (Larson, 1962; Aloni, 1987). This assertion is supported by the high correlation values recorded here between spring leaf and stem phenology in diffuse-porous species, but does not match with the capacity of ring-porous species to put on new wood before bud break. In ring-porous species, auxin or auxin precursors have been found in the cambial area prior to bud break (Savidge & Wareing, 1981). The presence of overwintering cambial derivatives has also been reported, and these wood cells can complete their maturation in spring prior to cambium reactivation (Zasada & Zahner, 1969; Frankenstein *et al.*, 2005). Debudding experiments also suggest the existence of alternative auxin sources readily available in dormant stem tissues of conifers (Little & Wareing, 1981; Sundberg & Uggla, 1998). Indeed, the radial growth onset of ring-porous *Quercus pubescens* and coniferous *Pinus sylvestris* and *Picea abies* in Europe revealed only small differences between ring-porous and coniferous trees ranging between one and two weeks (Zweifel *et al.*, 2006), similar to our observations.

The presence of wide earlywood vessels offers an enhanced water conductive capacity in spring relative to diffuse-porous and non-porous species, albeit at the cost of a higher risk of cavitation when water becomes scarce. Such trade-off suggests that ring porosity is a hydraulic strategy adapted to seasonal temperate climates (Gilbert, 1940; Lechowicz, 1984; Baas & Wheeler, 2011). Baas and Wheeler (2011) note an increasing number of ring-porous and semi-ring-porous species in the Northern Hemisphere since the Cretaceous, coincidental with the increasing seasonality of the climate in the area. Thus, early radial growth in ring-porous species is a probable adaptation to the severe loss of hydraulic conductivity suffered during late-summer water deficits and winter freeze-thaw events. Severe loss of hydraulic conductivity requires the formation of newly functional xylem cells to restore transpiration capacity prior to leaf-out (Sperry *et al.*, 1994; Hacke & Sauter, 1996), although some previous-year latewood vessels can remain functional the following year (Kudo *et al.*, 2018). Compared with ring-porous species, conifer tracheids and diffuse-porous vessels are very resistant to embolism. In the case of conifers, such resistance is required by their evergreen foliage which increases winter water losses (Hinckley & Lassoie, 1981). Conifers also differ from diffuse-porous species in that they can start photosynthesising using their existing foliage and reactivate their cambium as soon as spring conditions are suitable for growth (Hunter & Lechowicz, 1992; Wang *et al.*, 1992; Barbaroux & Bréda, 2002). The capacity of conifers to use older foliage is consistent with their later bud break, as observed here and documented in earlier studies (Hoch *et al.*, 2003; Michelot *et al.*, 2012). Diffuse-porous species also display a low vulnerability to embolism, limiting the need for early cambial reactivation (Hunter & Lechowicz, 1992; Sperry *et al.*, 1994). Compared to ring-porous species, the later cambial activity of diffuse-porous trees enables them to avoid using their stored carbohydrates for leaf flush, which may be better adapted to their indeterminate shoot growth pattern (Lechowicz, 1984). However, because wood growth in diffuse-porous species occurs later, this more conservative strategy of stored carbon use coincides with seasonal maxima in evapotranspiration and water deficit.

We found that diffuse-porous trees were exposed to several-fold higher levels of evapotranspiration and water deficit compared to other species, which likely is reflective of their resistance to embolism. In contrast, peak growth in co-occurring ring-porous and coniferous species was completed before this period. We can only speculate on the different adaptations that diffuse-species may have developed to compensate for this increased water deficit, such as reductions in leaf area, or increased carbon allocation to roots. Nonetheless, under the projected increase in drought frequency and intensity (Dai, 2013; Cook *et al.*, 2015), we argue that the strategy of later growth in diffuse-porous species may increase their drought vulnerability. This hypothesis is supported by multiple observations in Europe where ring-porous *Quercus robur*, *Q. rubra* and *Q. petraea* were found to be mainly sensitive to spring drought while diffuse-porous *Fagus sylvatica* was especially sensitive to summer drought (Michelot *et al.*, 2012; Vanhellemont *et al.*, 2019). In the Eastern U.S, diffuse-porous species have also been repeatedly reported to display stronger reductions in radial growth during and following years of extreme water deficit, as compared with ring-porous or non-porous species (Brzostek *et al.*, 2014; Elliott *et al.*, 2015; Kannenberg *et al.*, 2019). Similar patterns of response to interannual climate variability among ring-porous *Quercus* and *Carya* species also support the use of ring porosity as a functional group to help predict plant response to drought (Martin-Benito & Pederson, 2015).

Despite the reputation that manual dendrometer bands provide poorly-resolved growth estimates, our methodological approach, combined with the high sampling frequency and replication, provide a valid protocol to monitor intra-seasonal growth dynamics. In addition to the phenological observations discussed earlier, we also found a relatively high proportion of red maple trees displaying little to no annual stem growth. Such result confirms earlier observations of frequent missing growth rings for that species (Pederson, 2005; Pederson *et al.*, 2017). We also note the relatively weaker effect of tree size and vigor on the phenology of peak growth, relative to the genetically-driven wood structure. It is possible that traditional dendrometer bands could factor into these results. Our analytical approach, however, controlled for size and vigor effects on relative growth phenology, which masks the potential effect of phenological delays on total growth. Increased diameter growth has been previously observed to delay the ending of xylem maturation, thus extending the duration of wood formation (Lupi *et al.*, 2010). Our results confirm this previous finding. We should also point out that manual dendrometer bands measure girth increment, which is a coarse representation of the different stages of xylogenesis that is mostly influenced by the phase of cell enlargement (McMahon & Parker, 2015). As such, woody biomass production lags behind seasonal dynamics of stem girth increments (Cuny *et al.*, 2015). Thus, the dates of maximal stem growth discussed here may not represent the exact dates of peak cambial activity or carbon sequestration in the stem of the studied trees. Studies investigating high resolution growth of these species, such as conducted through microcoring (Deslauriers *et al.*, 2017), are vital to further understanding and refining the new results reported here.

Data and Materials Availability

The data that support this study are available online at http://harvardforest.fas.harvard.edu:8080/exist/apps/datasets/showData.html?id=hf069.

Supplementary Data

Note S1 Additional information on the prior distributions and Bayesian inferential approach used for statistical analysis.

Conflict of Interest

The authors declare no conflict of interest.

Funding

LD and NP acknowledge support from U.S Forest Service Northern Research Station (Joint Venture Agreement 17-JV-11242306-038), National Science Foundation Division of Environmental Biology Long-term Ecological Research (LTER; DEB-1832210). NP acknowledges support from the National Science Foundation Macrosystem Biology program (EF-1241930). ADR acknowledges support from the National Science Foundation (awards 1832210, 1741585, 1550740, and 1702697). Establishment and measurements on the biomass plots at the Harvard EMS was supported by U.S. Department of Energy, Office of Science through the National Institute of Global Environmental Change (NIGEC) and National Institute for Climate Change Research (NICCR) and are not part of the AmeriFlux Core Site network operated by the DOE Lawrence Berkeley Laboratory as well as by the National Science.

Acknowledgements

Foundation Long-Term Ecological Research program. Installation of the Harvard Forest biomass plots and dendrometer bands has taken the effort of many. We especially recognize Mike

Goulden, Carol Barford, Elizabeth Hammond-Pyle, and the many student participants in Research Experience for Undergraduate (REU) program at Harvard Forest that is supported by NSF. We would also like to thank Tim Whitby for his help with the processing of the dendroband data.

Authors' contribution

LD and NP designed the research; JWM led the collection of dendroband data, while JMD provided the estimates of atmospheric water demand; LD and MI conducted data analysis; LD and NP wrote the manuscript with significant input from all co-authors.

References

Allen CD, Breshears DD, McDowell NG. 2015. On underestimation of global vulnerability to tree mortality and forest die-off from hotter drought in the Anthropocene. *Ecosphere* 6: art129.

Aloni R. 1987. Differentiation of vascular tissues. *Annual Review of Plant Physiology* 38: 179–204.

Baas P, Wheeler EA. 2011. Wood anatomy and climate change. In: Climate Change, Ecology and Systematics. Cambridge University Press, 141–155.

Barbaroux C, Bréda N. 2002. Contrasting distribution and seasonal dynamics of carbohydrate reserves in stem wood of adult ring-porous sessile oak and diffuse-porous beech trees. *Tree Physiology* 22: 1201–1210.

Barford CC, Wofsy SC, Goulden ML, Munger JW, Pyle EH, Urbanski SP, Hutyra L, Saleska SR, Fitzjarrald D, Moore K. 2001. Factors Controlling Long- and Short-Term Sequestration of Atmospheric CO2 in a Mid-latitude Forest. *Science* 294: 1688–1691.

Bennett AC, McDowell NG, Allen CD, Anderson-Teixeira KJ. 2015. Larger trees suffer most during drought in forests worldwide. *Nature Plants* 1: 15139.

Berdanier AB, Clark JS. 2016. Multiyear drought-induced morbidity preceding tree death in southeastern U.S. forests. *Ecological Applications* 26: 17–23.

Bishop DA, Pederson N. 2015. Regional Variation of Transient Precipitation and Rainless-day Frequency Across a Subcontinental Hydroclimate Gradient. *Journal of Extreme Events* 02: 1550007.

Bonan GB. 2008. Forests and climate change: forcings, feedbacks, and the climate benefits of forests. *Science* 320: 144–1449.

Bottero A, D'Amato AW, Palik BJ, Bradford JB, Fraver S, Battaglia MA, Asherin LA. 2017. Density-dependent vulnerability of forest ecosystems to drought. *Journal of Applied Ecology* 54: 1605–1614.

Brzostek ER, Dragoni D, Schmid HP, Rahman AF, Sims D, Wayson CA, Johnson DJ, Phillips RP. 2014. Chronic water stress reduces tree growth and the carbon sink of deciduous hardwood forests. *Global Change Biology* 20: 2531–2539.

Buckland SM, Grime JP, Hodgson JG, Thompson K. 1997. A Comparison of Plant Responses to the Extreme Drought of 1995 in Northern England. *Journal of Ecology* 85: 875–882.

Buechling A, Martin PH, Canham CD. 2017. Climate and competition effects on tree growth in Rocky Mountain forests. *Journal of Ecology* 105: 1636–1647.

Cailleret M, Jansen S, Robert EMR, Desoto L, Aakala T, Antos Joseph A, Beikircher Barbara, Bigler Christof, Bugmann Harald, Caccianiga Marco, *et al.* 2017. A synthesis of radial growth patterns preceding tree mortality. *Global Change Biology* 23: 1675–1690.

Cook BI, Ault TR, Smerdon JE. 2015. Unprecedented 21st century drought risk in the American Southwest and Central Plains. *Science Advances* 1: 7.

Cuny HE, Rathgeber CBK, Frank D, Fonti P, Mäkinen H, Prislan P, Rossi S, del Castillo EM, Campelo F, Vavrčík H, *et al.* 2015. Woody biomass production lags stem-girth increase by over one month in coniferous forests. *Nature Plants* 1: 15160.

Dai A. 2013. Increasing drought under global warming in observations and models. *Nature Clim. Change* 3: 52–58.

D'Amato AW, Bradford JB, Fraver S, Palik BJ. 2013. Effects of thinning on drought vulnerability and climate response in north temperate forest ecosystems. *Ecological Applications* 23: 1735–1742.

Delpierre N, Vitasse Y, Chuine I, Guillemot J, Bazot S, Rutishauser T, Rathgeber CBK. 2016. Temperate and boreal forest tree phenology: from organ-scale processes to terrestrial ecosystem models. *Annals of Forest Science* 73: 5–25.

Denny EG, Gerst KL, Miller-Rushing AJ, Tierney GL, Crimmins TM, Enquist CAF, Guertin P, Rosemartin AH, Schwartz MD, Thomas KA, *et al.* 2014. Standardized phenology monitoring methods to track plant and animal activity for science and resource management applications. *International Journal of Biometeorology* 58: 591–601.

Deslauriers A, Fonti P, Rossi S, Rathgeber CBK, Gričar J. 2017. Ecophysiology and Plasticity of Wood and Phloem Formation. In: Amoroso MM, Daniels LD, Baker PJ, Camarero JJ, eds. Ecological Studies. Dendroecology: Tree-Ring Analyses Applied to Ecological Studies. Cham: Springer International Publishing, 13–33.

Deslauriers A, Morin H, Urbinati C, Carrer M. 2003. Daily weather response of balsam fir (*Abies balsamea* (L.) Mill.) stem radius increment from dendrometer analysis in the boreal forests of Québec (Canada). *Trees* 17: 477–484.

Deslauriers A, Rossi S, Anfodillo T. 2007. Dendrometer and intra-annual tree growth: What kind of information can be inferred? *Dendrochronologia* 25: 113–124.

Deslauriers A, Rossi S, Anfodillo T, Saracino A. 2008. Cambial phenology, wood formation and temperature thresholds in two contrasting years at high altitude in southern Italy. *Tree Physiology* 28: 863–871.

D'Orangeville L, Côté B, Houle D, Morin H. 2013a. The effects of throughfall exclusion on xylogenesis of balsam fir. *Tree Physiology* 33: 516–526.

D'Orangeville L, Côté B, Houle D, Morin H, Duchesne L. 2013b. A three-year increase in soil temperature and atmospheric N deposition has minor effects on the xylogenesis of mature balsam fir. *Trees - Structure and Function* 27: 1525–1536.

D'Orangeville L, Maxwell J, Kneeshaw D, Pederson N, Duchesne L, Logan T, Houle D, Arseneault D, Beier CM, Bishop DA, *et al.* 2018. Drought timing and local climate determine the sensitivity of eastern temperate forests to drought. *Global Change Biology* 24: 2339–2351.

Dyer JM. 2009. Assessing topographic patterns in moisture use and stress using a water balance approach. *Landscape Ecology* 24: 391–403.

Elliott KJ, Miniat CF, Pederson N, Laseter SH. 2015. Forest tree growth response to hydroclimate variability in the southern Appalachians. *Global Change Biology* 21: 4627–4641.

Forner A, Valladares F, Bonal D, Granier A, Grossiord C, Aranda I, Mencuccini M. 2018. Extreme droughts affecting Mediterranean tree species' growth and water-use efficiency: the importance of timing. *Tree Physiology* 38: 1127–1137.

Foster TE, Schmalzer PA, Fox GA. 2014. Timing matters: the seasonal effect of drought on tree growth. *The Journal of the Torrey Botanical Society* 141: 225–241.

Frankenstein C, Eckstein D, Schmitt U. 2005. The onset of cambium activity - A matter of agreement? *Dendrochronologia* 23: 57–62.

Gelman A, Carlin JB, Stern HS, Dunson DB, Vehtari A, Rubin DB. 2013. *Bayesian Data Analysis*. Chapman and Hall/CRC.

Gilbert SG. 1940. Evolutionary Significance of Ring Porosity in Woody Angiosperms. *Botanical Gazette* 102: 105–120.

Gleason KE, Bradford JB, Bottero A, D'Amato AW, Fraver S, Palik BJ, Battaglia MA, Iverson L, Kenefic L, Kern CC. 2017. Competition amplifies drought stress in forests across broad climatic and compositional gradients. *Ecosphere* 8: e01849-n/a.

Grossiord C. 2018. Having the right neighbors: how tree species diversity modulates drought impacts on forests. *New Phytologist* 0.

Gruber A, Strobl S, Veit B, Oberhuber W. 2010. Impact of drought on the temporal dynamics of wood formation in *Pinus sylvestris*. *Tree Physiology* 30: 490–501.

Hacke U, Sauter JJ. 1996. Xylem Dysfunction during Winter and Recovery of Hydraulic Conductivity in Diffuse-Porous and Ring-Porous Trees. *Oecologia* 105: 435–439.

Hinckley TM, Lassoie J. 1981. Radial growth in conifers and deciduous trees: A comparison. *Mitteilungen der forstlichen Bundesversuchsanstalt Wien* 142: 17–56.

Hoch G, Richter A, KÖRner C. 2003. Non-structural carbon compounds in temperate forest trees. *Plant, Cell & Environment* 26: 1067–1081.

Huang M, Wang X, Keenan TF, Piao S. 2018. Drought timing influences the legacy of tree growth recovery. *Global Change Biology* 24: 3546–3559.

Hunter AF, Lechowicz MJ. 1992. Predicting the timing of budburst in temperate trees. *The Journal of Applied Ecology* 29: 597.

Itter MS, D'Orangeville L, Dawson A, Kneeshaw D, Duchesne L, Finley AO. 2019. Boreal tree growth exhibits decadal-scale ecological memory to drought and insect defoliation, but no negative response to their interaction. *Journal of Ecology* 0: 1:14.

Jenkins JC, Chojnacky DC, Heath LS, Birdsey RA. 2004. Comprehensive database of diameter-based biomass regressions for North American tree species. *Gen. Tech. Rep. NE-319. Newtown Square, PA: U.S. Department of Agriculture, Forest Service, Northeastern Research Station. 45 p. [1 CD-ROM]*. 319.

Kannenberg SA, Maxwell JT, Pederson N, D'Orangeville L, Ficklin DL, Phillips RP. 2019. Drought legacies are dependent on water table depth, wood anatomy and drought timing across the eastern US. *Ecology Letters* 22: 119–127.

Kozlowski TT, Winget CH. 1964. Diurnal and seasonal variation in radii of tree stems. *Ecology* 45: 149–155.

Kudo K, Utsumi Y, Kuroda K, Yamagishi Y, Nabeshima E, Nakaba S, Yasue K, Takata K, Funada R. 2018. Formation of new networks of earlywood vessels in seedlings of the deciduous ring-porous hardwood Quercus serrata in springtime. *Trees* 32: 725–734.

Larson PR. 1962. Auxin gradients and the regulation of cambial activity. In: Kozlowski TT, ed. Tree Growth. New York: The Ronald Press Company, 97–117.

Larson PR. 1994. *The Vascular Cambium: Development and Structure*. Berlin Heidelberg: Springer-Verlag.

Lavigne MB, Little CHA, Riding RT. 2004. Changes in stem respiration rate during cambial reactivation can be used to refine estimates of growth and maintenance respiration. *New Phytologist* 162: 81–93.

Lechowicz MJ. 1984. Why Do Temperate Deciduous Trees Leaf Out at Different Times? Adaptation and Ecology of Forest Communities. *The American Naturalist* 124: 821–842.

Lempereur M, Martin-StPaul NK, Damesin C, Joffre R, Ourcival J-M, Rocheteau A, Rambal S. 2015. Growth duration is a better predictor of stem increment than carbon supply in a Mediterranean oak forest: implications for assessing forest productivity under climate change. *New Phytologist* 207: 579–590.

Little CHA, Wareing PF. 1981. Control of cambial activity and dormancy in *Picea sitchensis* by indol-3-ylacetic and abscisic acids. *Canadian Journal of Botany* 59: 1480–1493.

Lupi C, Morin H, Deslauriers A, Rossi S. 2010. Xylem phenology and wood production: resolving the chicken-or-egg dilemma. *Plant, Cell & Environment*.

Martin-Benito D, Kint V, del Río M, Muys B, Cañellas I. 2011. Growth responses of West-Mediterranean Pinus nigra to climate change are modulated by competition and productivity: Past trends and future perspectives. *Forest Ecology and Management* 262: 1030–1040.

Martin-Benito D, Pederson N. 2015. Convergence in drought stress, but a divergence of climatic drivers across a latitudinal gradient in a temperate broadleaf forest. *Journal of Biogeography* 42: 925–937.

McDowell NG, Allen CD. 2015. Darcy's law predicts widespread forest mortality under climate warming. *Nature Clim. Change* 5: 669–672.

McMahon SM, Parker GG. 2015. A general model of intra-annual tree growth using dendrometer bands. *Ecology and Evolution* 5: 243–254.

Michelot A, Bréda N, Damesin C, Dufrêne E. 2012. Differing growth responses to climatic variations and soil water deficits of Fagus sylvatica, Quercus petraea and Pinus sylvestris in a temperate forest. *Forest Ecology and Management* 265: 161–171.

Padilla FM, Pugnaire FI. 2007. Rooting depth and soil moisture control Mediterranean woody seedling survival during drought. *Functional Ecology* 21: 489–495.

Pan Y, Birdsey RA, Fang J, Houghton R, Kauppi PE, Kurz WA, Phillips OL, Shvidenko A, Lewis SL, Canadell JG, *et al.* 2011. A Large and Persistent Carbon Sink in the World's Forests. *Science* 333: 988–993.

Pederson N. 2005. Climatic Sensitivity and Growth of Southern Temperate Tress in the Eastern US: Implicatins for the Carbon Cycle.

Pederson N, Young A, Stan AB, Ariya U, Martin-Benito. 2017. Low-hanging DendroDynamic Ecological Fruits Regarding Disturbance in Temperate, Mesic Forests. In: Amoroso M, Daniels L, Baker P, Camarero JJ, eds. Dendroecology: Tree-ring Analyses Applied to Ecological Studies. Springer.

Peters W, Velde IR van der, Schaik E van, Miller JB, Ciais P, Duarte HF, Laan-Luijkx IT van der, Molen MK van der, Scholze M, Schaefer K, *et al.* 2018. Increased water-use efficiency and reduced CO 2 uptake by plants during droughts at a continental scale. *Nature Geoscience* 11: 744.

Phillips RP, Ibáñez I, D'Orangeville L, Hanson PJ, Ryan MG, McDowell NG. 2016. A belowground perspective on the drought sensitivity of forests: Towards improved understanding and simulation. *Forest Ecology and Management* 380: 309–320.

605 Priestley JH, Scott LI. 1936. A note upon summer wood production in the tree. *Proceedings of* 606 *the Leeds Philosophical and Literary Society* 3: 235–248.

607 Rathgeber CBK, Rossi S, Bontemps J-D. 2011. Cambial activity related to tree size in a mature 608 silver-fir plantation. *Annals of Botany* 108: 429–438.

609 Richardson AD. 2019. Tracking seasonal rhythms of plants in diverse ecosystems with digital 610 camera imagery. *New Phytologist* 222: 1742–1750.

611 Richardson AD, O'Keefe J. 2009. Phenological Differences Between Understory and Overstory: 612 A Case Study Using the Long-Term Harvard Forest Records. In: Phenology of Ecosystem 613 Processes. New York: Springer Science + Business, 87–117.

614 Rossi S, Deslauriers A, Anfodillo T. 2006a. Assessment of cambial activity and xylogenesis by 615 microsampling tree species: an example at the alpine timberline. *IAWA Journal* 27: 383–394.

616 Rossi S, Deslauriers A, Anfodillo T, Carrer M. 2008a. Age-dependent xylogenesis in timberline 617 conifers. *New Phytologist* 177: 199–208.

618 Rossi S, Deslauriers A, Anfodillo T, Morin H, Saracino A, Motta R, Borghetti M. 2006b. 619 Conifers in cold environments synchronize maximum growth rate of tree-ring formation with 620 day length. *New Phytologist* 170: 301–310.

621 Rossi S, Deslauriers A, Gricar J, Seo JW, Rathgeber CBK, Anfodillo T, Morin H, Levanic T, 622 Oven P, Jalkanen R. 2008b. Critical temperatures for xylogenesis in conifers of cold climates. 623 *Global Ecology and Biogeography* 17: 696–707.

624 Sass-Klaassen U, Sabajo CR, den Ouden J. 2011. Vessel formation in relation to leaf phenology in pedunculate oak and European ash. *Dendrochronologia* 29: 171–175.

626 Savidge RA, Wareing PF. 1981. Plant growth regulators and the differentiation of vascular elements. In: Barnett JR, ed. Xylem cell development. London: Castle House, 192–235.

628 Seftigen K, Frank DC, Björklund J, Babst F, Poulter B. 2018. The climatic drivers of normalized difference vegetation index and tree-ring-based estimates of forest productivity are spatially coherent but temporally decoupled in Northern Hemispheric forests. *Global Ecology and Biogeography* 27: 1352–1365.

632 Sengupta M, Xie Y, Lopez A, Habte A, Maclaurin G, Shelby J. 2018. The National Solar Radiation Data Base (NSRDB). *Renewable and Sustainable Energy Reviews* 89: 51–60.

634 Smith WB, Brand GJ. 1983. Allometric Biomass Equations for 98 Species of Herbs, Shrubs, and Small Trees. *Research Note NC-299. St. Paul, MN: U.S. Dept. of Agriculture, Forest Service, North Central Forest Experiment Station* 299.

637 Sperry JS, Nichols KL, Sullivan JEM, Eastlack SE. 1994. Xylem Embolism in Ring-Porous, Diffuse-Porous, and Coniferous Trees of Northern Utah and Interior Alaska. *Ecology* 75: 1736–1752.

640 Sundberg B, Uggla C. 1998. Origin and dynamics of indoleacetic acid under polar transport in *Pinus sylvestris*. *Physiologia Plantarum* 104: 22–29.

642 Suzuki M, Yoda K, Suzuki H. 1996. Phenological Comparison of the Onset of Vessel Formation
643 Between Ring-Porous and Diffuse-Porous Deciduous Trees in a Japanese Temperate Forest.
644 *IAWA journal*.

645 Takahashi S, Okada N, Nobuchi T. 2013. Relationship between the timing of vessel formation
646 and leaf phenology in ten ring-porous and diffuse-porous deciduous tree species. *Ecological*
647 *Research* 28: 615–624.

648 Tardif J, Flannigan M, Bergeron Y. 2001. An Analysis of the Daily Radial Activity of 7 Boreal
649 Tree Species, Northwestern Quebec. *Environmental Monitoring and Assessment* 67: 141–160.

650 Trugman AT, Detto M, Bartlett MK, Medvigy D, Anderegg WRL, Schwalm C, Schaffer B,
651 Pacala SW. 2018. Tree carbon allocation explains forest drought-kill and recovery patterns.
652 *Ecology Letters* 21: 1552–1560.

653 Vanhellemont M, Sousa-Silva R, Maes SL, Van den Bulcke J, Hertzog L, De Groote SRE, Van
654 Acker J, Bonte D, Martel A, Lens L, *et al.* 2019. Distinct growth responses to drought for oak
655 and beech in temperate mixed forests. *Science of The Total Environment* 650: 3017–3026.

656 Wang J, Ives NE, Lechowicz MJ. 1992. The relation of foliar phenology to xylem embolism in
657 trees. *Functional Ecology* 6: 469–475.

658 Wareing PF. 1951. Growth Studies in Woody Species IV. The Initiation of Cambial Activity in
659 Ring-Porous Species. *Physiologia Plantarum* 4: 546–546.

West AG, Dawson TE, February EC, Midgley GF, Bond WJ, Aston TL. 2012. Diverse functional responses to drought in a Mediterranean-type shrubland in South Africa. *New Phytologist* 195: 396–407.

Williams AP, Allen CD, Macalady AK, Griffin D, Woodhouse CA, Meko DM, Swetnam TW, Rauscher SA, Seager R, Grissino-Mayer HD, *et al.* 2013. Temperature as a potent driver of regional forest drought stress and tree mortality. *Nature Clim. Change* 3: 292–297.

Wyckoff PH, Clark JS. 2000. Predicting tree mortality from diameter growth: a comparison of maximum likelihood and Bayesian approaches. *Canadian Journal of Forest Research* 30: 156–167.

Wyckoff PH, Clark JS. 2002. The relationship between growth and mortality for seven co-occurring tree species in the southern Appalachian Mountains. *Journal of Ecology* 90: 604–615.

Zasada JC, Zahner R. 1969. Vessel element development in the earlywood of red oak (Quercus rubra). *Canadian Journal of Botany* 47: 1965–1971.

Zimmermann MH, Brown CL. 1971. *Trees: Structure and Function*. Berlin Heidelberg: Springer-Verlag.

Zweifel R, Zimmermann L, Zeugin F, Newbery DM. 2006. Intra-annual radial growth and water relations of trees: implications towards a growth mechanism. *Journal of Experimental Botany* 57: 1445–1459.

List of figures

Figure 1. Location of the 34 study plots and the EMS eddy-flux tower at Harvard Forest (a) and within Eastern North America (b). Linear features (e.g. roads, former agricultural stone walls) are in grey.

Figure 2. Example of the logistic growth model fitted on diameter measurements (DBH) taken on a yellow birch in 1999. Dotted lines indicate the day of year when modelled growth reached 25, 50, 75, and 100% of its cumulative annual value. The inset figure shows the daily growth rate for that tree derived from the fitted model.

Figure 3. Wood and leaf phenology over 1999-2003 across individuals (red curves) and averaged per species (coloured symbols). Error bars indicate 95% credible intervals (stem phenology) or standard deviation (leaf phenology). W25: 25% of annual radial growth; W50: 50% of annual radial growth; W75: 75% of annual radial growth; BB: bud break; L75: leaf out. (a) Daily modelled growth of all 1992 tree-years. Black lines indicate 10^{th}, 50^{th} and 90^{th} quantiles of daily growth rates. (b) Posterior mean estimates of wood phenology per species. Average leaf phenology measured at the site for corresponding species and years is also presented when available.

Figure 4. Wood and leaf phenology averaged per diffuse-porous, ring-porous or non-porous wood type. Error bars indicate 95% credible interval (stem phenology) or standard deviation (leaf phenology), while ribbons indicate 10^{th} and 90^{th} percentile values. W25: 25% of annual radial growth; W50: 50% of annual radial growth; W75: 75% of annual radial growth; BB: bud break; L75: leaf development. (a) Standardized diameter increment. (b) Standardized daily growth rate. (c) Posterior mean estimates of wood phenology. Corresponding leaf phenology averaged over the study period is also presented. (d) Posterior mean estimates of growth duration (days between 25% and 75% growth).

Figure 5. Posterior mean estimated effect of tree biomass and vigor (standardized units) on the Julian day when 50% of growth is completed according to wood structure, with all other variables held constant at their median value. Coloured ribbons indicate 95% credible intervals for the posterior mean.

Figure 6. Covariation between wood phenology indices and (a) bud break and (b) leaf out among (black) and within (coloured) species per wood structure types. Error bars indicate standard deviation from the mean. W25: 25% of annual radial growth; W50: 50% of annual radial growth; W75: 75% of annual radial growth. The leaf phenology of the species included in the analysis is averaged over 3-5 individuals (species represented by a single individual were excluded).

Figure 7. Climatic conditions at our study site (a) over the study period (1999-2003), during modelled peak growth averaged per wood structure type (b) per year and (c) over the study period, and (d) over a longer period, 1998-2014.

716 **Table 1.** Summary of sampled trees. Diffuse-porous, non-porous and ring-porous represent 49,
717 26 and 25% of trees, respectively.

Species	No. of trees	No. of plots	Mean biomass (kg C) [5th,95th]	Vigor (%) [5th,95th]	Wood structure
Striped maple	5	1	21 [16-27]	2.3 [0.9-4.5]	Diffuse-porous
Red maple	222	34	89 [19-245]	1.3 [0.1-3.3]	Diffuse-porous
Yellow birch	33	15	79 [21-228]	1.8 [0.1-4.1]	Diffuse-porous
Black birch	9	6	173 [29-623]	2.4 [0.6-3.8]	Diffuse-porous
White birch	5	4	158 [60-346]	0.7 [0.1-1.8]	Diffuse-porous
Grey birch	7	2	107 [55-178]	1.0 [0.2-2.1]	Diffuse-porous
American beech	8	6	89 [25-180]	2.8 [0.9-5.4]	Diffuse-porous
Black cherry	13	7	291 [35-768]	0.7 [0-1.5]	Diffuse-porous
White spruce	23	4	48 [22-86]	0.5 [0-0.9]	Non-porous
Red pine	31	3	211 [81-353]	1.1 [0.3-2.0]	Non-porous
Eastern white pine	27	10	170 [25-455]	1.7 [0.3-3.3]	Non-porous
Eastern hemlock	77	14	113 [14-334]	2.2 [0.2-4.8]	Non-porous
White ash	12	5	249 [67-433]	0.9 [0.1-1.9]	Ring-porous
Northern red oak	125	31	418 [88-1204]	1.7 [0.5-2.9]	Ring-porous
Black oak	13	10	275 [54-548]	2.3 [0.7-5.3]	Ring-porous
TOTAL	**610**	**34**	**180 [20-631]**	**1.5 [0.1-3.8]**	

718

719

720

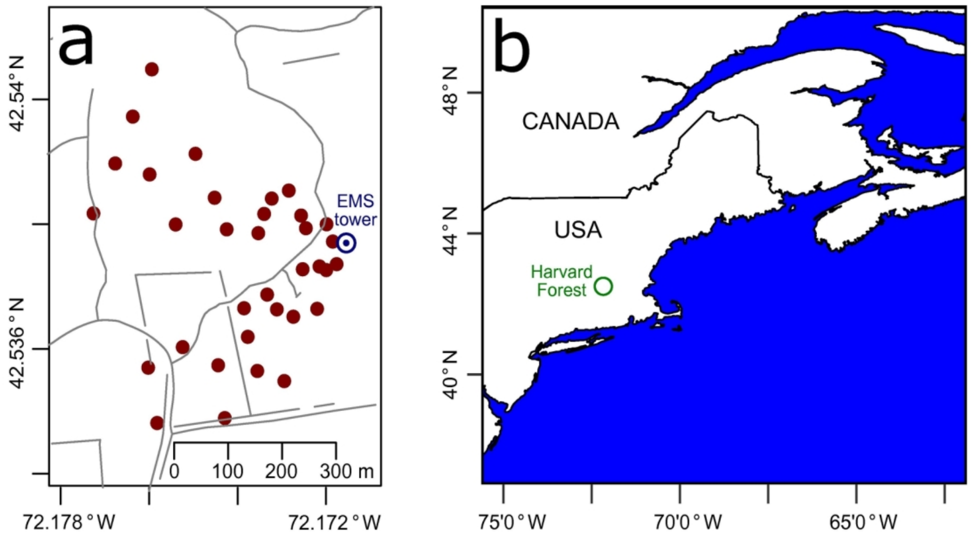

Figure 1. Location of the 34 study plots and the EMS eddy-flux tower at Harvard Forest (a) and within Eastern North America (b). Linear features (e.g. roads, former agricultural stone walls) are in grey.

150x82mm (300 x 300 DPI)

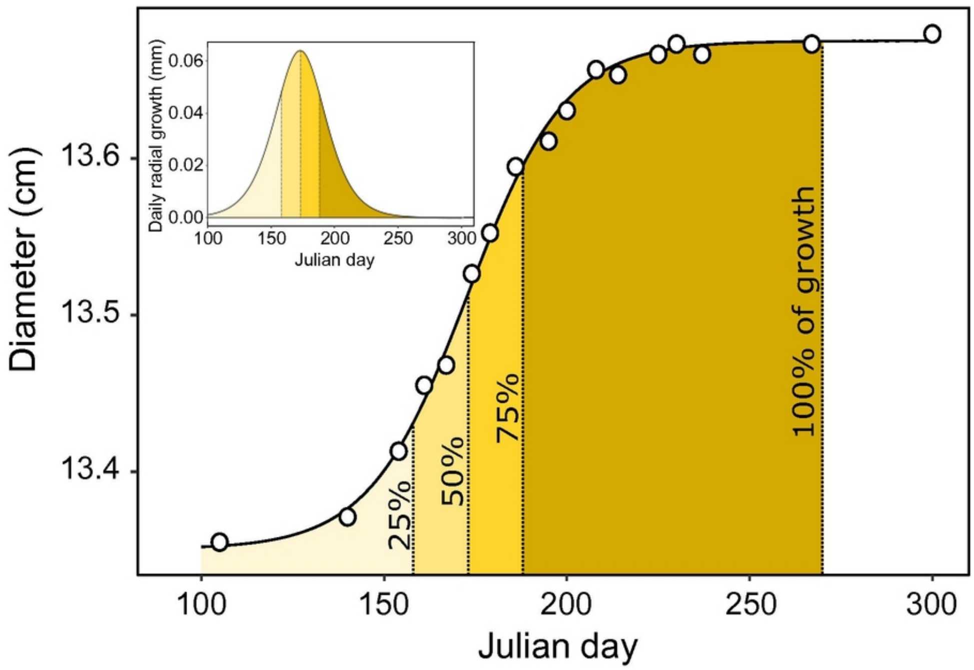

Figure 2. Example of the logistic growth model fitted on diameter measurements (DBH) taken on a yellow birch in 1999. Dotted lines indicate the day of year when modelled growth reached 25, 50, 75, and 100% of its cumulative annual value. The inset figure shows the daily growth rate for that tree derived from the fitted model.

78x54mm (300 x 300 DPI)

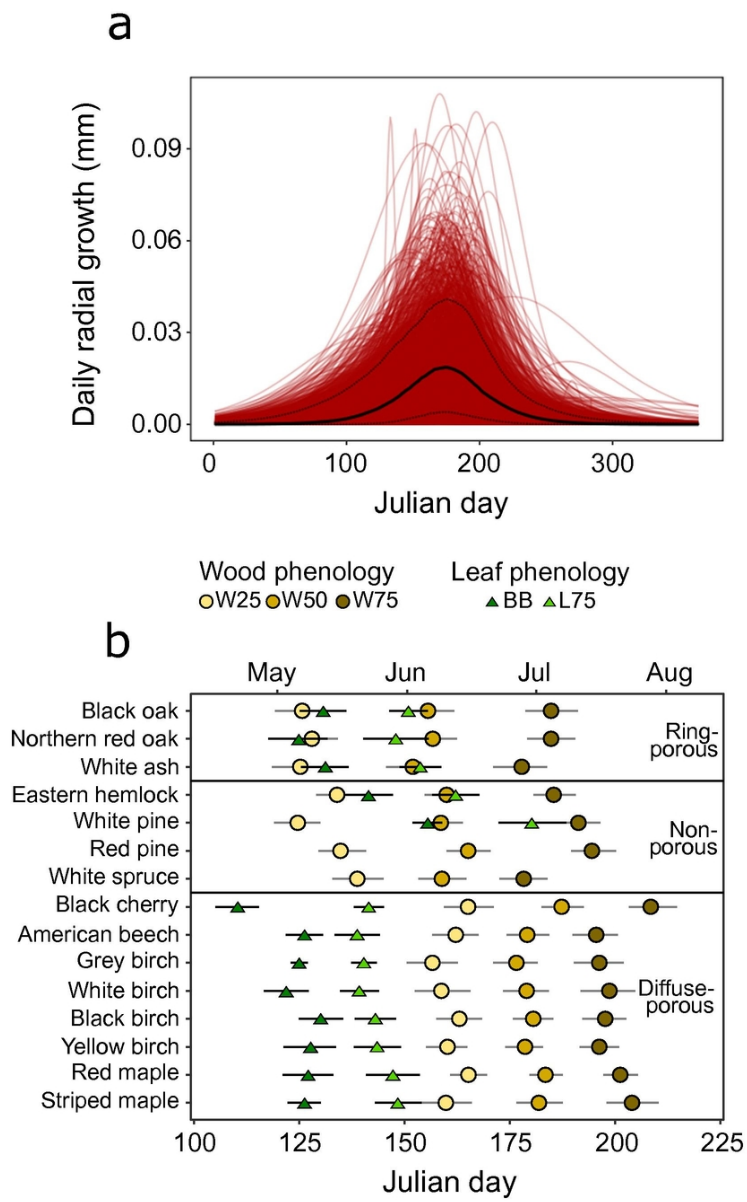

Figure 3. Wood and leaf phenology over 1999-2003 across individuals (red curves) and averaged per species (coloured symbols). Error bars indicate 95% credible intervals (stem phenology) or standard deviation (leaf phenology). W25: 25% of annual radial growth; W50: 50% of annual radial growth; W75: 75% of annual radial growth; BB: bud break; L75: leaf out. (a) Daily modelled growth of all 1992 tree-years. Black lines indicate 10th, 50th and 90th quantiles of daily growth rates. (b) Posterior mean estimates of wood phenology per species. Average leaf phenology measured at the site for corresponding species and years is also presented when available.

71x113mm (300 x 300 DPI)

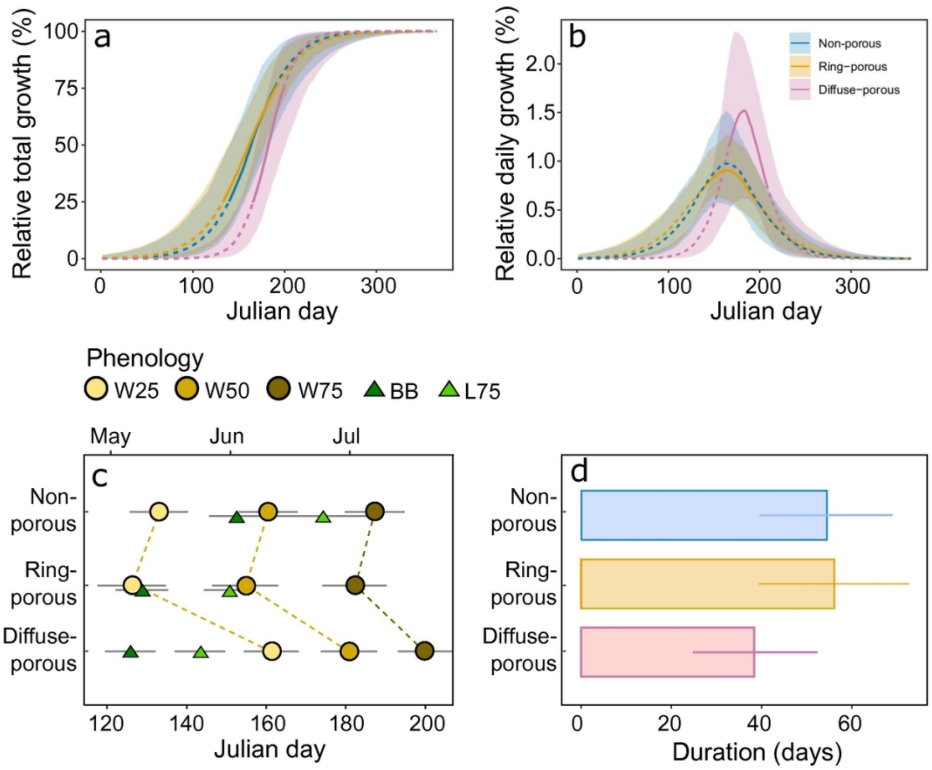

Figure 4. Wood and leaf phenology averaged per diffuse-porous, ring-porous or non-porous wood type. Error bars indicate 95% credible interval (stem phenology) or standard deviation (leaf phenology), while ribbons indicate 10th and 90th percentile values. W25: 25% of annual radial growth; W50: 50% of annual radial growth; W75: 75% of annual radial growth; BB: bud break; L75: leaf development. (a) Standardized diameter increment. (b) Standardized daily growth rate. (c) Posterior mean estimates of wood phenology. Corresponding leaf phenology averaged over the study period is also presented. (d) Posterior mean estimates of growth duration (days between 25% and 75% growth).

113x88mm (300 x 300 DPI)

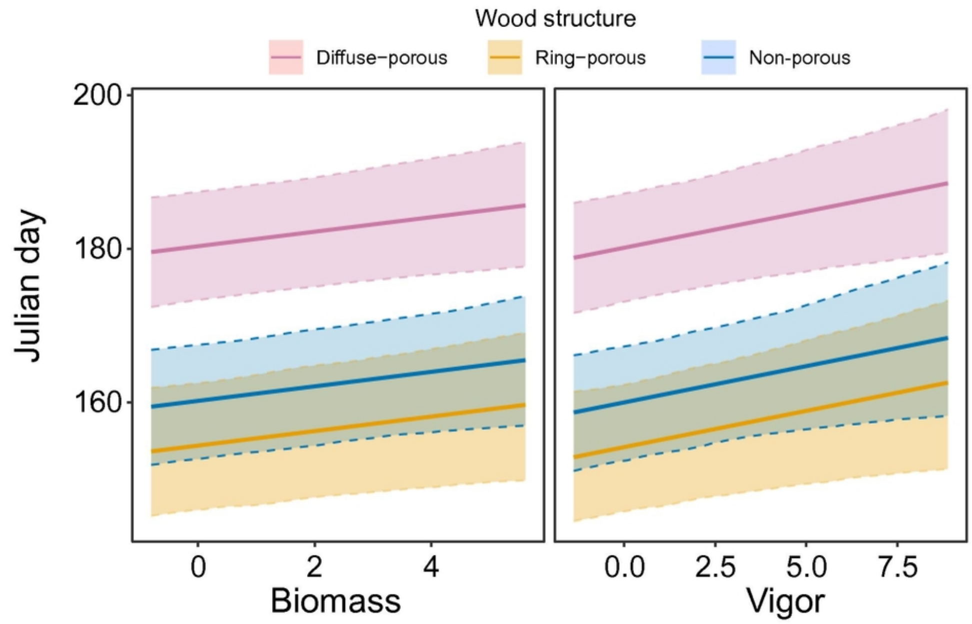

Figure 5. Posterior mean estimated effect of tree biomass and vigor (standardized units) on the Julian day when 50% of growth is completed according to wood structure, with all other variables held constant at their median value. Coloured ribbons indicate 95% credible intervals for the posterior mean.

82x54mm (300 x 300 DPI)

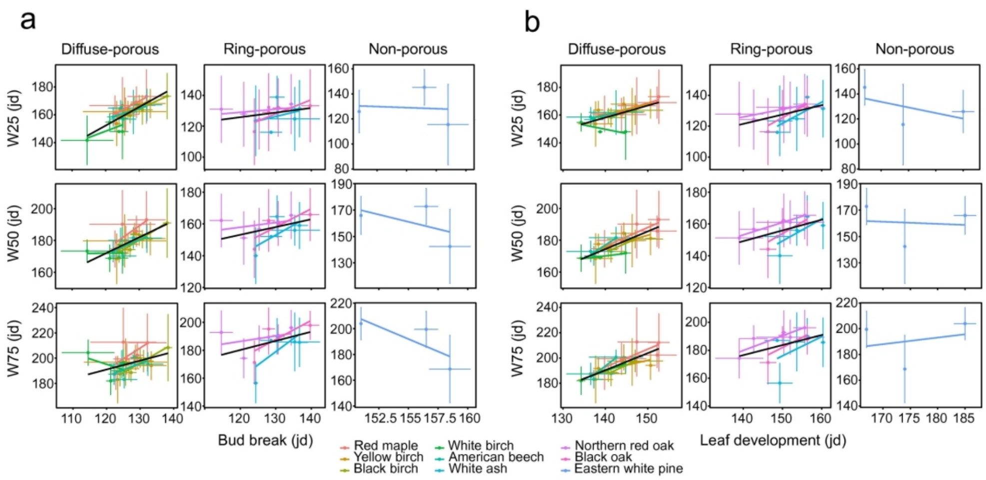

Figure 6. Covariation between wood phenology indices and (a) bud break and (b) leaf out among (black) and within (coloured) species per wood structure types. Error bars indicate standard deviation from the mean. W25: 25% of annual radial growth; W50: 50% of annual radial growth; W75: 75% of annual radial growth. The leaf phenology of the species included in the analysis is averaged over 3-5 individuals (species represented by a single individual were excluded).

186x92mm (300 x 300 DPI)

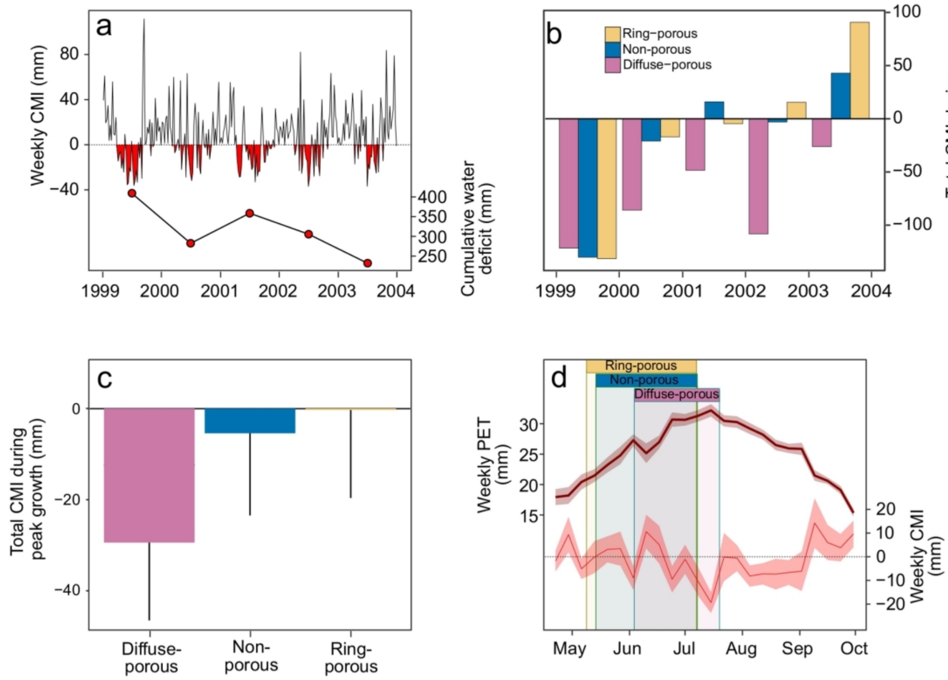

Figure 7. Climatic conditions at our study site (a) over the study period (1999-2003), during modelled peak growth averaged per wood structure type (b) per year and (c) over the study period, and (d) over a longer period, 1998-2014.

160x113mm (300 x 300 DPI)